

Effect of gas evolution on current distribution and ohmic resistance in a vertical cell under forced convection conditions

YOSHINORI NISHIKI

Research and Development Center, Permelec Electrode Ltd., 1159, Ishikawa, Fujisawa, Kanagawa prefecture, 252 Japan

KOICHI AOKI, KOICHI TOKUDA, HIROAKI MATSUDA

Department of Electronic Chemistry, Graduate School at Nagatsuta, Tokyo Institute of Technology, Nagatsuta, Midori-ku, Yokohama, 227 Japan

Received 22 July 1985; revised 7 September 1985

The volume fraction of gas bubbles in a vertical cell with a separator was evaluated on the basis of the Bruggemann equation by taking into account the increase in velocity of the rising gas bubbles when fresh solution without gas bubbles is supplied to the bottom of the cell at constant velocity. This enhancement of the velocity results from an increase in the volume of gases evolving at the working electrode. The following three cases for overpotential at the working electrode were considered: no overpotential, overpotential of the linear type and of the Butler-Volmer type. The volume fraction, ε_h , at the top of the cell was expressed as a function of the dimensionless height of the cell and kinetic parameters. The total cell resistance can be expressed by $\{(2/5\varepsilon_h)[(1 - \varepsilon_h)^{-3/2} - 1 + \varepsilon_h] + \mu\} \rho_1 d_1 / wh$, where ρ_1 is the resistivity of the solution without gas bubbles, d_1 the interelectrode distance, w the cell width, h the cell height and μ the parameter involving overpotential and resistance of the separator. It was found that there is an optimum value of the interelectrode distance. The optimum value is about a quarter of the value for the case of constant gas rise velocity, which corresponds to a closed system.

Nomenclature

b	linear overpotential coefficient	R_t	total cell resistance
C	proportionality constant given by Equation 2	T	temperature
d_1	interelectrode distance	u	auxiliary function defined by Equation 37
d_2	thickness of the separator	v	solution velocity in the cell
F	Faraday constant	v_0	solution velocity at the bottom of the cell
h	height of the cell	v_h	solution velocity at the top of the cell
i	current density	V	voltage at the working electrode
I	total current	V_{eq}	voltage at the working electrode when no current flows
i_0	exchange current density	w	width of the electrode
k	parameter given by $d_1(z)^{1/2}$	y	axis in the vertical direction from the bottom of the cell
n	number of electrons transferred	z	dimensionless variable for y , defined by Equation 8
p	gas pressure	z_h	dimensionless variable for h , defined by $[C(V - V_{eq})/(\rho_1 d_1 v_0)]h$
r	dimensionless cell resistance defined by Equation 16		
R	gas constant		

α	anodic transfer coefficient in the Butler–Volmer equation	μ_L or $\mu_S + \mu_{BV}$	μ_L or $\mu_S + \mu_{BV}$
ε	volume fraction of gas bubbles in the cell	μ_L	ratio defined by Equation 41
ε_h	volume fraction of gas bubbles at the top of the cell	μ_S	ratio defined by $b/(\rho_1 d_1)$
ζ	dimensionless cell voltage, given by Equation 38	ρ_1	ratio defined by $\rho_2 d_2/(\rho_1 d_1)$
η	Butler–Volmer overpotential	$\rho_1(y)$	resistivity of the solution phase without gas bubbles
η'	Butler–Volmer overpotential when current density, I/wh , flows through the electrode, as described in Equation 42	ρ_2	resistivity of the solution phase with gas bubbles at level y
μ	parameter representing either μ_S , $\mu_S +$	Λ	resistivity of the separator
			kinetic parameter in the Butler–Volmer equation, given by Equation 39

1. Introduction

Industrial electrolysis in production-type cells is almost always accompanied by gas evolution. Evolving gases alter both the ohmic drop of the solution and mass transport in the cell. Several models for effects of gas evolution have been reviewed by Vogt [1].

The relation between the effective conductivity of the solution involving gas bubbles and the volume fraction of gas bubbles has been investigated on the basis of Maxwell's and Bruggemann's equations [1]. The relation has been tested experimentally with suspensions of solid particles [2, 3] and with dispersion of simulated gas evolution [4]. Tanaka *et al.* [5] exaggerated the presence of the bubble-dispersion layer of chlorine gas by measuring the variation of potential with the distance between the electrode and a probe. Hine *et al.* [6] considered non-uniform bubble distribution, in which gas dispersion was concentrated near the electrode and more dilute in the bulk. Sides and Tobias [7] calculated the potential field around a spherical bubble in contact with an electrode and then examined it experimentally [8]. Vogt [9] derived an expression for the ohmic interelectrode resistance on the assumption of uniform current distribution in the cell with a bubble curtain. Lanzi and Savinell [10] presented a two-dimensional constriction model of a dense bubble curtain.

Tobias [11] applied Bruggemann's equation to estimating the effect of gas evolution on current distribution in a vertical cell composed of a parallel plate electrode. Nagy [12] calculated the current distribution in a cell with vertical blade electrodes, according to the treatment of Tobias [11]. In these two reports, a stagnant electrolyte was assumed. In industrial cells, however, it is common to supply electrolytes to the cell [1] by forced convection or natural circulation. Under this condition, Funk and Thorpe [13] and Thorpe *et al.* [14] extended the theory to the more complicated system of water electrolysis. Rousar *et al.* [15, 16] carried out a chemical engineering calculation for a chlorate cell by combining various parameters. Since this previous work has been devoted to evaluating operating factors, the fundamental relation between current distribution and volume fraction of gases has been left unsolved.

The target of this work is to discuss systematically these effects by evaluating cell resistance as a function of volume fraction of gas bubbles evolved at a parallel plate electrode in a vertical cell with a separator on the basis of the Bruggemann equation under the condition of forced convection. The following three cases for overpotential at the working electrode are considered: no overpotential, overpotential of the linear type and of the Butler–Volmer type.

2. Assumptions and basic equations

We consider a vertical cell equipped with working and counter electrodes between which a separator (e.g. an ion exchange membrane or a diaphragm) is inserted, as depicted in Fig. 1. The following assumptions are made:

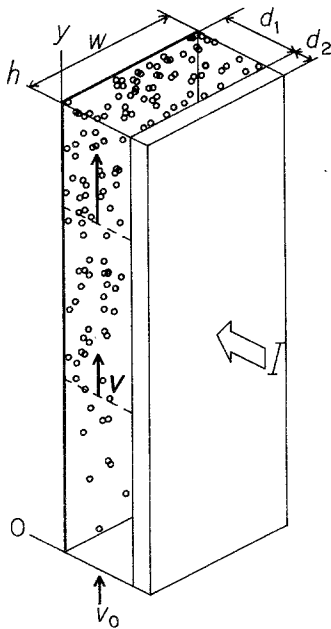


Fig. 1. Geometry of the model cell and schematic representation of distribution of evolving gas bubbles.

(a) The height of the cell is larger than the distance between the working electrode and the separator so that the flow of current can be regarded as unidirectional and perpendicular to the electrode.

(b) The working electrode and the counter electrode have such a good conductance that each electrode has equipotential distribution.

(c) There is no overpotential at the counter electrode. In addition the interstice between the counter electrode and the separator is so narrow that the interface between the separator and the interstice has equipotential distribution. Therefore our concern is directed to a compartment involving the working electrode.

(d) We take the distance along the electrode from the bottom of the cell to be y . Then the ohmic resistivity, $\varrho_1(y)$, of the solution involving gas bubbles with the volume fraction, $\varepsilon(y)$, at the level y is given by the Bruggemann equation [17]

$$\varrho_1(y) = \varrho_1[1 - \varepsilon(y)]^{-3/2} \quad (1)$$

where ϱ_1 denotes the resistivity of the solution when the solution does not contain any bubbles. The validity of Equation 1 has been verified experimentally when spherical insulators with a large size-range are dispersed randomly in a conductive solution [2, 3]. Equation 1 has been applied extensively to the estimation of the conductivity of solutions mixed with gas bubbles.

(e) Gas bubbles are generated only by the electrode reaction and the generation rate is proportional to the current density at the working electrode.

(f) Gas bubbles thus generated are immediately unidirectionally dispersed in the cell toward the separator and hence there is no variation of gas fraction in the direction perpendicular to the working electrode.

(g) Bubble-free solution is supplied to the bottom of the cell. The inlet velocity, v_0 , is externally controlled so that it is independent of the height of the cell and the fraction of the gas bubbles.

(h) The velocity of gas bubbles relative to that of the solution is neglected. This relative velocity which is caused by buoyancy is much smaller than the inlet velocity commonly employed in industrial electrolysis [13, 14]. This assumption is equivalent to the fact that the slip ratio is unity.

(i) There is no variation of the pressure over the cell.

(j) Solution flows with a uniform velocity distribution in the direction perpendicular to the electrode.

The equation for the mass balance [18] of gas bubbles under steady state conditions is given by

$$d(\varepsilon v)/dy = Ci \quad (2)$$

The complement of the volume fraction of gas bubbles becomes the volume fraction of the solution, expressed by $(1 - \varepsilon)$. Since there is no sink or source of the solution except at the inlet and the outlet of the cell, the equation for mass balance of the solution in the cell is expressed by

$$d[(1 - \varepsilon)v]/dy = 0 \quad (3)$$

The boundary condition at $y = 0$ is given by

$$\varepsilon(0) = 0 \quad \text{and} \quad v(0) = v_0 \quad (4)$$

Integrating Equation 3 under Condition 4 yields

$$v = v_0/(1 - \varepsilon) \quad (5)$$

Adding Equation 2 to Equation 3 and eliminating v by use of Equation 5 leads to

$$i = (v_0/C)(1 - \varepsilon)^{-2}(d\varepsilon/dy) \quad (6)$$

This is a basic equation which gives the relation between the current density and the volume fraction of gas bubbles. If a current-potential relation at the working electrode is specified, the volume fraction of gas bubbles can be evaluated by combining the current-potential equation with Equations 1 and 6. The current-potential relations treated here are those of no overpotential, of the linear type and the Butler-Volmer type. The effective voltage applied between the working electrode and the counter electrode is taken to be $V - V_{\text{eq}}$.

3. Current distribution and ohmic resistance

3.1. No overpotential

In the absence of overpotential at the working electrode, the resistance of the interelectrode gap at the level y is expressed by $[q_1(y)d_1 + q_2d_2]$, where $q_1(y)$ varies with the volume fraction of gas bubbles and hence is a function of y . Then the current density is given by

$$i = (V - V_{\text{eq}})/[q_1(y)d_1 + q_2d_2] \quad (7)$$

Eliminating $q_1(y)$ from Equations 1 and 7, inserting the resulting equation into Equation 6 and introducing the following dimensionless variable:

$$z = [C(V - V_{\text{eq}})/(q_1d_1v_0)]y \quad (8)$$

we obtain

$$dz/d\varepsilon = (1 - \varepsilon)^{-7/2} + \mu_s(1 - \varepsilon)^{-2} \quad (9)$$

where

$$\mu_s = q_2d_2/(q_1d_1) \quad (10)$$

The solution of Equation 9 with the condition $\varepsilon(0) = 0$ is given by

$$z = (2/5)[(1 - \varepsilon)^{-5/2} - 1] + \mu_s\varepsilon/(1 - \varepsilon) \quad (11)$$

When there is no separator in the cell, i.e. $\mu_s = 0$, an explicit solution for ε can be obtained from Equation 11 in the following form:

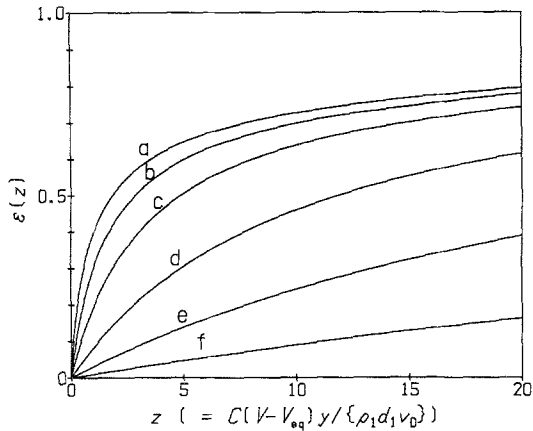


Fig. 2. Variation of volume fraction of gas bubbles with dimensionless cell height for $\mu_s =$ (a): 0, (b): 1, (c): 3, (d): 10, (e): 30 and (f): 100.

$$\epsilon = 1 - [(1 + (5z/2))]^{-2/5} \tag{12}$$

In Fig. 2, variations of $\epsilon(z)$ with z are shown for several values of μ_s . The linear variation found at large values of μ_s is ascribed to the resistance of the separator being much larger than that of the solution. For small values of μ_s , ϵ increases markedly with z and then tends to the curve calculated from Equation 12. As $z \rightarrow \infty$, ϵ approaches unity.

In Fig. 3, the distribution of the dimensionless current density, $i[(\rho_1 d_1)/(V - V_{eq})]$, being equal to $(d\epsilon/dz)(1 - \epsilon)^{-2}$ or $1/[(1 - \epsilon)^{-3/2} + \mu_s]$, is shown for several values of μ_s . From comparison of these curves, one can easily see that the current distribution becomes uniform and the current density becomes small as the value of μ_s increases. Thus μ_s is a significant factor determining the current distribution. The curves in Fig. 3 may provide some measure of the durability of the electrode because durability is closely related to the current density.

The variation of the velocity of the solution with the dimensionless height of the cell is expressed implicitly by

$$z = (2/5)[(v/v_0)^{5/2} - 1] + \mu_s(v/v_0 - 1) \tag{13}$$

which has been derived by eliminating ϵ from Equations 5 and 11. For $\mu_s = 0$, v/v_0 is given by

$$v/v_0 = (1 + 5z/2)^{2/5} \tag{14}$$

In Fig. 4, the variations are shown for several values of μ_s . A linear variation of v/v_0 with z for sufficiently large values of μ_s is shown. With a decrease in μ_s , acceleration of the velocity is enhanced.

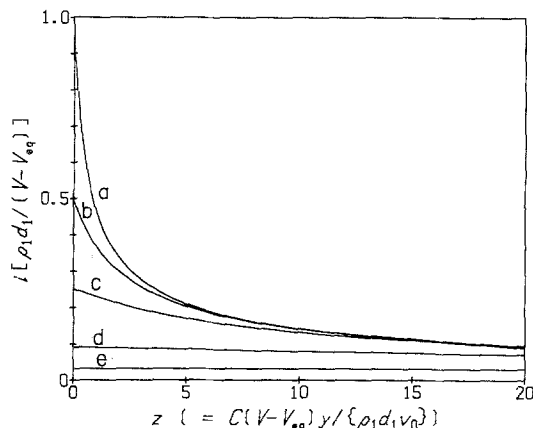


Fig. 3. Distribution of current density on the working electrode for $\mu_s =$ (a): 0, (b): 1, (c): 3, (d): 10 and (e): 30.

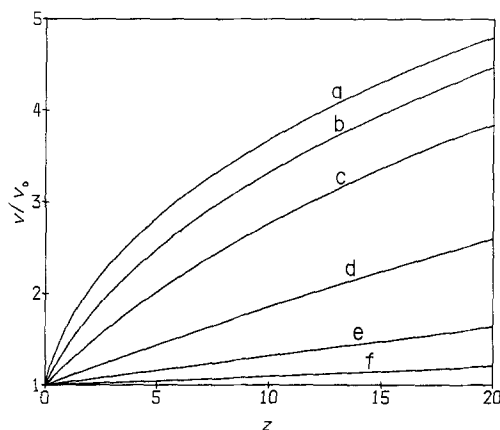


Fig. 4. Variation of solution velocity with z for $\mu_s =$ (a): 0, (b): 1, (c): 3, (d): 10, (e): 30 and (f): 100.

For $\mu_s = 0$, the solution velocity increases considerably and varies as $z^{2/5}$ because of the large variation of ε with z , as shown in Curve (a) of Fig. 2. However in real cells, this rapid increase in v may be reduced by an increase in the pressure of the gas and the solution viscosity.

The most significant characteristic of the cell is the total cell resistance, R_t , defined by

$$R_t = (V - V_{eq})/I \quad (15)$$

Then the dimensionless cell resistance, r , is given by

$$r = (V - V_{eq})wh/(Iq_1 d_1) = R_t wh/(q_1 d_1) \quad (16)$$

r can be expressed as a function of ε using the following procedures. Integration of Equation 2 yields

$$CI = \varepsilon_h v_h w \quad (17)$$

from which v_h is eliminated by use of Equation 5. Then it follows that

$$I = w(v_0/C)\varepsilon_h/(1 - \varepsilon_h) \quad (18)$$

Inserting this equation into Equation 16 yields

$$r = z_h(1 - \varepsilon_h)/\varepsilon_h \quad (19)$$

Inserting Equation 11 into Equation 19 results in

$$r = (2/5\varepsilon_h)[(1 - \varepsilon_h)^{-3/2} - 1 + \varepsilon_h] + \mu \quad (20)$$

where μ_s has been replaced by μ , which stands for either μ_s , $\mu_s + \mu_L$ or $\mu_s + \mu_{BV}$, because it will be shown that this equation is still valid for $\mu_s + \mu_L$ or $\mu_s + \mu_{BV}$. The first term on the right hand side represents the resistance of the solution including gas bubbles, while the last term denotes the resistance of the separator. Therefore the dimensionless cell resistance can be expressed by a simple sum of dimensionless resistances of the solution phase and of the separator. In Fig. 5, values of $r - \mu$ are plotted against ε_h . When values of ε_h are small, expanding Equation 20 about $\varepsilon_h = 0$ yields

$$r - \mu = 1 + (3/4)\varepsilon_h + (7/8)\varepsilon_h^2 + \dots \quad (21)$$

From this equation, a rough estimation of the increase in the resistivity of the solution phase due to gas bubbles is given by $(3/4)\varepsilon_h$. When the value of ε_h approaches unity, the resistance of the solution phase increases rapidly. However it is unimportant to discuss the behaviour for ε_h -values near unity because it is questionable whether the Bruggemann equation is valid for this range of ε_h .

Tobias [11] derived an expression for the volume fraction of gas bubbles in a closed cell without forced convection of the solution. The conditions employed were formally equivalent to

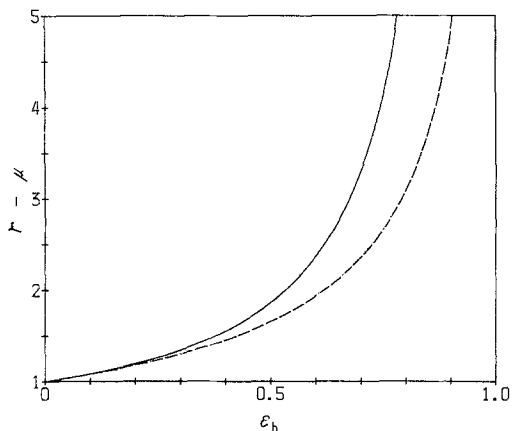


Fig. 5. Variation of the dimensionless cell resistance with ε_h for $\mu = 0$. The solid curve, calculated from Equation 20, corresponds to the open system with forced convection while the dashed curve, calculated from Equation 22, corresponds to the closed system without forced convection, which has been evaluated by Tobias.

independence of bubble rise velocity from height of the cell, i.e. taking v in Equation 2 to be constant, v_0 . Inserting Equation 2 written in terms of v_0 into Equation 7, combining with Equation 1 and integrating the resulting equation yields

$$z_h = 2[(1 - \varepsilon_h)^{-1/2} - 1] + \mu\varepsilon_h \quad (22)$$

Values of $r - \mu$, calculated from the combination of Equations 19 and 22, are plotted against ε in Fig. 5 as a dashed curve. When the dashed curve is compared with the solid curve at the same value on the ordinate in Fig. 5, it is noted that the volume fraction in the cell without forced convection is larger than that with forced convection due to the fact that the solution velocity is not increased.

It is of interest to express R_i as a function of d_1 . Since bubbles generated by electrode reactions are assumed to be dispersed uniformly over the interelectrode region, the constant C is inversely proportional to d_1 . Hence z_h can be reduced to

$$z_h = k^2/d_1^2 \quad (23)$$

where k is independent of d_1 . Combining Equations 12 for $\mu_s = 0$ and 19 yields

$$R_i wh/\rho_1 = (k/d_1)/\{[1 + 2.5(k/d_1)^2]^{2/5} - 1\} \quad (24)$$

Variations of $R_i wh/\rho_1$ with d_1/k are shown as the solid Curve (a) in Fig. 6. When values of d_1/k are very large, $R_i wh/\rho_1$ approaches the asymptotic (dotted) line, $R_i wh/\rho_1 = d_1/k$, which would be observed without gas bubbles. With a decrease in d_1/k , the curve gradually deviates upwards and rises suddenly after passing through the minimum point. For $d_1/k < 0.04$, it is found from Equation

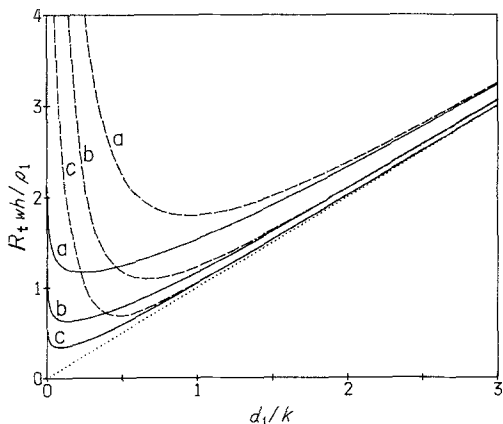


Fig. 6. Dependence of the cell voltage on the interelectrode distance. The solid curve, calculated from Equation 24, corresponds to the open system with forced convection while the dashed curve corresponds to the closed system without forced convection, which has been evaluated by Tobias. The dotted line denotes the asymptotic line in the case of no bubble evolution. These curves are for $\mu =$ (a): 0, (b): 1 and (c): 3.

24 that $R_t wh/\rho_1$ is inversely proportional to $d_1^{1/5}$. The increase results from an increase in the resistivity in the interelectrode gap caused by the accumulation of gas bubbles. The appearance of the minimum implies that there is an optimum interelectrode distance. This value is $d_1/k = 0.238$. If gas bubbles are generated at 100% current efficiency and can be regarded to behave ideally, the volume of gas generated by a current density i is expressed by $(i/nF)(RT/p)$. Then the proportionality constants C and k are given by

$$C = (1/nF)(RT/p)/d_1 \quad (25)$$

and

$$k = [RT(V - V_{eq})h/(nFp\rho_1 v_0)]^{1/2} \quad (26)$$

respectively. Therefore the optimum interelectrode distance, $(d_1)_{opt}$, is given by

$$(d_1)_{opt} = 0.238[RT(V - V_{eq})h/(nFp\rho_1 v_0)]^{1/2} \quad (27)$$

Tobias found the presence of an optimum value of the interelectrode distance and evaluated the value for the case of stagnant electrolytes [11]. Since his derivation contained unnecessary assumptions, Nagy corrected the optimum value [16] to give $d_1/k = 0.944$. Comparing this value with 0.238 indicates that forced convection reduces the optimum value by a factor of approximately 4.

Values of $R_t wh/\rho_1$ for $\mu \neq 0$ are shown in Fig. 6. Since it was difficult to derive an explicit form of $R_t wh/\rho_1$, we evaluated $R_t wh/\rho_1$ numerically. With an increase in μ , the curves shift downward and to the left because a large part of the cell resistance is due to the resistance of the separator. Then values of $(d_1)_{opt}$ become smaller. We examined the variation of $(d_1)_{opt}$ with μ and obtained the following approximate equations:

$$(d_1)_{opt} = 0.238k/(1 + 0.65\mu^{0.87}) \quad (28)$$

The corresponding minimum cell resistance, r_{min} , is approximately given by

$$r_{min} = 1.17k\rho_1/(1 + 0.9\mu^{0.9}) \quad (29)$$

Errors involved in Equations 28 and 29 are less than 3%.

3.2. Overpotential varying linearly with the current density

When the overpotential is expressed by a linear relation to the current density, the cell resistance at the level y is given by $[b + \rho_1(y)d_1 + \rho_2 d_2]$. Then the current density becomes

$$i(y) = (V - V_{eq})/[b + \rho_1(y)d_1 + \rho_2 d_2] \quad (30)$$

If $\rho_2 d_2$ in Equation 7 is replaced by $(b + \rho_2 d_2)$ in Equation 30, Equation 30 is equivalent to Equation 7. Since both b and $\rho_2 d_2$ are independent of y , Equations 9, 11, 12 and 20 with replacement of $\rho_2 d_2$ by $b + \rho_2 d_2$ are also valid for the case of this overpotential, where μ is, instead of Equation 10, given by

$$\mu = \mu_L + \mu_S = (b + \rho_2 d_2)/(\rho_1 d_1) \quad (31)$$

$$\mu_L = b/(\rho_1 d_1) \quad (32)$$

μ_L is a parameter expressing the leveling effect [11]. By taking into account this replacement, every equation in Section 3.1 is valid. The reason for permitting this simple replacement is that the coefficient b is equivalent to ohmic resistance.

Combination of Equations 20 and 31 shows that the total cell resistance is a series connection of the ohmic drop and the resistance due to overpotential. Therefore the ratio χ of the overpotential to the ohmic drop is given by

$$\begin{aligned} \chi &= \mu_L / \{ (2/5\varepsilon_h) [(1 - \varepsilon_h)^{-3/2} - 1 + \varepsilon_h] + \mu_S \} \\ &= b / \{ \rho_1 d_1 (2/5\varepsilon_h) [(1 - \varepsilon_h)^{-3/2} - 1 + \varepsilon_h] + \rho_2 d_2 \} \end{aligned} \quad (33)$$

This is the same as the Wagner number for the case in which ohmic resistance increases due to evolution of gas bubbles.

3.3. Overpotential subject to the Butler–Volmer equation

The Butler–Volmer equation, excluding effects of concentration variations, is given by

$$i = i_0 \{ \exp(\alpha n F \eta / RT) - \exp[(\alpha - 1)n F \eta / RT] \} \quad (34)$$

Then the cell voltage is expressed by the sum of the overpotential and the ohmic drop in the following form:

$$V - V_{eq} = \eta + i[\rho_1(y)d_1 + \rho_2 d_2] \quad (35)$$

Eliminating η from Equations 34 and 35, inserting Equations 1 and 6 into the resulting equation and changing variable y for z by use of Equation 8 yields

$$(\zeta/\Lambda)(1 - \varepsilon)^{-2}(d\varepsilon/dz) = \exp(\alpha \zeta u) - \exp[(\alpha - 1)\zeta u] \quad (36)$$

where

$$u = 1 - [(1 - \varepsilon)^{-3/2} + \mu_s](1 - \varepsilon)^{-2}(d\varepsilon/dz) \quad (37)$$

$$\zeta = nF(V - V_{eq})/RT \quad (38)$$

$$\Lambda = nFi_0 \rho_1 d_1 / RT \quad (39)$$

Equations 36 and 37 show that the function $\varepsilon(z)$ has four parameters, μ_s , ζ , Λ and α . Since Equation 36 is a differential equation with a non-linear relation with respect to $d\varepsilon/dz$, it is very difficult to obtain an analytical solution for $\varepsilon(z)$. Hence we evaluated $\varepsilon(z)$ numerically. The numerical procedure employed was as follows: Equations 36 and 37, into which the initial condition $\varepsilon(0) = 0$ was inserted, were solved with respect to $(d\varepsilon/dz)_{z=0}$ by use of the Newton method. From the value of $(d\varepsilon/dz)_{z=0}$ thus evaluated, the Runge–Kutta method [19] permitted evaluation of $\varepsilon(\Delta z)$, from which $(d\varepsilon/dz)_{z=\Delta z}$ was determined again from Equations 36 and 37, where Δz is an infinitesimal value of z . Further application of the Runge–Kutta method yielded a value of $\varepsilon(2\Delta z)$. Iterating according to this procedure led to numerical values of $\varepsilon(z)$ for four parameters.

In Fig. 7, values of r or those of $z_h(1 - \varepsilon_h)/\varepsilon_h$ thus computed are plotted against ε_h for five values of ζ at $\mu_s = 0$, $\alpha = 0.5$ and $\Lambda = 0.2$. Curve (A), being for the largest value of ζ in Fig. 7, is almost the same as the curve calculated from Equation 20 at $\mu = 0$. This consistency results from the fact that the contribution of the ohmic drop to the total cell voltage is predominant compared to that of the overpotential for large values of the cell voltage or the current density, as shown in Fig. 2 in

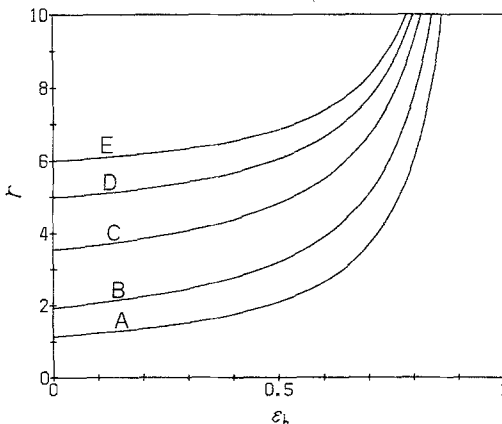


Fig. 7. Variation of the dimensionless cell resistance with ε_h for $\mu_s = 0$, $\Lambda = 0.2$ and $\zeta =$ (A): 100, (B): 15, (C): 6, (D): 3 and (E): 0.2 when overpotential is of the Butler–Volmer type.

the previous paper [20]. In other words, the current distribution at large values of ζ is the primary one. Conversely when ζ approaches zero, values of r tend to the curve from Equation 20 which is shifted upward by Λ^{-1} . This amount of shift corresponds to the dimensionless resistance of the linearized Butler–Volmer equation for small values of ζ . Therefore Curve (E) in Fig. 7 is in good agreement with the curve calculated from Equation 20 in which μ is replaced by Λ^{-1} . For intermediate values of ζ , the curves are similar to Curve (A) which is shifted upward by the amount of the increase in the resistance due to the overpotential. This amount varies with Λ , ζ , μ_s and ε_h in a complex manner.

When one estimates the cell resistance, it may be helpful to have a simple approximate equation capable of expressing variations of r with ε_h . Examining these variations for many combinations of parameters, α , Λ , ζ and μ_s with ε_h , we found that Equation 20 holds approximately when μ is given by

$$\mu = \mu_s + \mu_{BV} = \varrho_2 d_2 / (\varrho_1 d_1) + [\eta' wh / (I \varrho_1 d_1)] \quad (40)$$

$$\mu_{BV} = \eta' wh / (I \varrho_1 d_1) \quad (41)$$

Here η' denotes the dimensionless overpotential calculated from the Butler–Volmer equation when current I flows through the cell without gas bubbles:

$$I / (i_0 hw) = \exp(\alpha n F \eta' / RT) - \exp[(\alpha - 1) n F \eta' / RT] \quad (42)$$

The error involved in Equation 20 in which μ is replaced by $(\mu_s + \mu_{BV})$ is less than 3% for any value of ζ , Λ , μ_s , $0 \leq \varepsilon_h \leq 0.8$ and $0.1 \leq \alpha \leq 0.9$. By taking into account the replacement given by Equation 40, Equations 20–22, 24, 27–29 including r in Section 3.1 are still valid for the case of the Butler–Volmer overpotential.

When Equation 20 is multiplied by $I \varrho_1 d_1$, the following current–voltage expression is obtained:

$$V - V_{eq} = (I/wh) \varrho_1 d_1 \{ (2/5 \varepsilon_h) [(1 - \varepsilon_h)^{-3/2} - 1 + \varepsilon_h] + \mu_s \} + \eta' \quad (43)$$

The first term on the right hand side of Equation 43 expresses the total ohmic drop in the cell while the second term represents the overpotential when a current density, I/wh , flows through the electrode without gas bubbles. The cell voltage can be expressed by the simple sum of the ohmic drop and the overpotential. Therefore the ratio of the overpotential to the ohmic drop is given by

$$\chi = \eta' / [(I/wh) \varrho_1 d_1 \{ (2/5 \varepsilon_h) [(1 - \varepsilon_h)^{-3/2} - 1 + \varepsilon_h] \} + \mu_s] \quad (44)$$

In the case of the Butler–Volmer equation, χ is different from the Wagner number because it varies intricately with current [20].

Distributions of ε , v/v_0 and i along the electrode surface can be roughly estimated from the curves in Figs 2, 3 and 4, respectively when μ_s is replaced by $\mu_s + \mu_{BV}$. However it was found that variations of ε , v/v_0 and i with z are larger than those for the case of linear overpotential at the same value of μ , especially at the bottom of the cell. In other words, the leveling effect in the Butler–Volmer case is smaller than that in the linear case.

Acknowledgement

The authors wish to express their appreciation for fruitful suggestions by Mr Seiji Nakagawa, President, Permelec Electrode Ltd.

References

- [1] H. Vogt, 'A Comprehensive Treatise of Electrochemistry', Vol. 6 (edited by E. Yeager, J. O'M. Bockris, B. Conway and S. Surangapai) Plenum, New York (1981).
- [2] J. C. R. Turner, *Chem. Engng Sci.* **31** (1976) 487.

- [3] R. E. De La Rue and C. W. Tobias, *J. Electrochem. Soc.* **106** (1959) 827.
- [4] L. Sigrist, O. Dossenbach and N. Ibl, *J. Appl. Electrochem.* **10** (1980) 223.
- [5] K. Tanaka, H. Morishita and Y. Kihara, *Denkikagaku (J. Electrochem. Soc. Jpn)* **32** (1964) 378.
- [6] F. Hine, M. Yasuda, R. Nakamura and T. Noda, *J. Electrochem. Soc.* **122** (1975) 1185.
- [7] P. J. Sides and C. W. Tobias, *ibid.* **127** (1980) 288.
- [8] *Idem, ibid.* **129** (1982) 2715.
- [9] H. Vogt, *Electrochim. Acta* **26** (1981) 1311.
- [10] O. Lanzi and R. F. Savinell, *J. Electrochem. Soc.* **130** (1983) 799.
- [11] C. W. Tobias, *ibid.* **106** (1959) 833.
- [12] Z. Nagy, *J. Appl. Electrochem.* **6** (1976) 171.
- [13] J. E. Funk and J. F. Thorpe, *J. Electrochem. Soc.* **116** (1969) 48.
- [14] J. F. Thorpe, J. E. Funk and T. Y. Bong, *J. Basic Engng* **92** (1970) 173.
- [15] I. Rousar, *J. Electrochem. Soc.* **116** (1969) 676.
- [16] I. Rousar, V. Cezner, J. Nejeppsava, M. M. Jaksic, M. Spasojevic and B. Z. Nikolic, *J. Appl. Electrochem.* **7** (1977) 427.
- [17] D. A. D. Bruggemann, *Ann. Phys.* **24** (1935) 636.
- [18] R. Haase, 'Thermodynamics of Irreversible Processes', Addison-Wesley Publishing Company, Massachusetts (1969) pp. 224-8.
- [19] M. Abramowitz and I. A. Stegun, 'Handbook of Mathematical Functions', Dover Publications, New York (1965) p. 896.
- [20] Y. Nishiki, K. Aoki, K. Tokuda and H. Matsuda, *J. Appl. Electrochem.*, in press.